Subwavelength interference with an effective entangled source

Peilong Hong and Guoquan Zhang*

The MOE Key Laboratory of Weak Light Nonlinear Photonics and School of Physics, Nankai University, Tianjin 300457, China

(Received 23 May 2013; published 25 October 2013)

We propose a two-photon subwavelength interference scheme for classical light in which multiple quantum-like entangled two-photon paths play an essential role. These entangled two-photon paths are introduced through a specially designed source composed of many point sources j with j's complex amplitude being a superposition of modes $e^{i\phi_j}$ and $e^{i\phi_j^{(1)}}$, where ϕ_j and $\phi_j^{(1)}$ are temporally random phases but satisfying $\phi_j + \phi_j^{(1)} = \phi_0$, with ϕ_0 being either a constant or a random phase in time. Interference between the entangled two-photon paths could lead to second-order subwavelength interference of an object put in front of the source plane. In a proof-of-principle experiment, by using a spatial light modulator to modulate the wave front of a coherent light, we have generated such a source and observed subwavelength interference of a double-slit mask via two-photon measurement.

DOI: 10.1103/PhysRevA.88.043838 PACS number(s): 42.50.St, 07.60.Ly, 42.25.Hz, 42.50.Ar

I. INTRODUCTION

Due to the wave property of light, the spatial resolution of an imaging system is limited by the wavelength of light, which is usually known as the Rayleigh criterion [1]. Interestingly, the limitation is allowed to be broken in quantum mechanics with the idea of the photonic de Broglie wave. The de Broglie wave, which is one of the key concepts in quantum theory, shows that a particle could behave like a wave with a wavelength of $\lambda = h/p$, where h is the Planck constant and p is the momentum of the particle. It is obvious that the de Broglie wavelength would decrease as the momentum of the particle increases. Based on this, by introducing a conceptual "effective" beam splitter which could bind photons together, Jacobson *et al.* expanded the de Broglie wave into optical physics, proposing the photonic de Broglie wave [2]. The key of the photonic de Broglie wave is that if multiple photons behave as a whole one, the wavelength of the multiphoton unit will become shorter, leading to subwavelength interference. Then the problem is how one can bind multiple photons together in practice since photons are identical bosons with no interaction between them during their propagation in free space.

Now, it is well known that the signature of bound N photons is the appearance of an entangled state. The first observation of the photonic de Broglie wave was reported with the entangled two-photon state generated through a parametric down-conversion process [3,4]. It was also realized that subwavelength interference with the entangled two-photon source is useful for lithography with a resolution higher than the classical diffraction limit by a factor of 2 [5,6]. To achieve higher-order subwavelength interference, an entangled multiphoton state is needed, and a widely employed one is the two-path NOON state: $(|N,0\rangle_{A,B} + |0,N\rangle_{A,B})/\sqrt{2}$. With such a state, Nth-order subwavelength interference could be realized between the two entangled paths A and B, which could lead to superresolving phase measurement [7–9]. In this stage, the applications of subwavelength interference with quantum entangled sources are seriously limited since generation of the quantum state is difficult in practice and the generated quantum field is also very weak.

To overcome the limitation of the quantum field, several methods have been developed to realize subwavelength interference with a classical light. One way is to achieve second-order subwavelength interference of an object in the Hanbury Brown and Twiss (HBT) setup [10]. However, in a conventional HBT-type setup, two-photon measurement is done with two detectors scanning in the opposite directions, indicating the realized subwavelength interference is not applicable in practice. Recently, it was found that the flaw could be overcome with a modified HBT-type setup, in which an incoherent interferometer is inserted so that the intensity correlation between a pair of symmetric positions at the input port of the incoherent interferometer is transferred to the correlation of the same position between two orthogonally polarized modes at the output port [11]. Other methods show that subwavelength interference could also be realized by considering the optical nonlinearity of material [12,13] or by a postselected measurement [14,15].

In this paper, with a specially designed classical source, we report a NOON-type subwavelength interference of an object in a linear scheme, which theoretically relies on the photonic de Broglie wave and is experimentally observed without any postselected operation.

II. MODEL AND PRINCIPLE

To explain how we realize a two-photon de Broglie wave with a classical light, let's first recall the quantum interpretation of the HBT-type two-photon interference with phase-independent source, which relies on the superposition of two indistinguishable two-photon paths [16–19]. For a traditional phase-independent source, such as a thermal light, the complex amplitude of its jth ($j = 1,2,3,\ldots$) point sources is proportional to $e^{i\phi_j}$, where ϕ_j is an independent and temporally random phase. Considering two photons from a pair of independent point sources (1,2) that trigger a coincidence count, there are two alternative indistinguishable two-photon paths, as shown in Fig. 1(a): Photon s_1 (empty circle) goes to detector D1 while photon s_2 (solid circle) goes to detector D2 and vice versa. The amplitudes of two-photon paths are proportional to $e^{i(\phi_1+\phi_2)}e^{i\phi_{s\to D}}$, with $e^{i\phi_{s\to D}}$ being the temporally stable propagation phase for the pair of photons traveling

*zhanggq@nankai.edu.cn

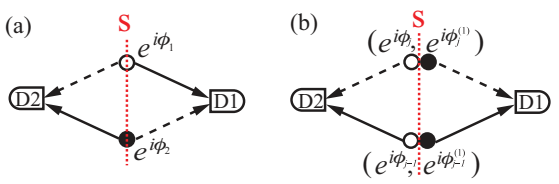

FIG. 1. (Color online) (a) Unfold scheme of the HBT-type twin indistinguishable two-photon paths for a pair of photons occupying two modes of two different point sources. (b) Unfold scheme of the NOON-type two-photon paths for a pair of photons occupying two modes of the same point source [the dashed and the solid lines are for the jth and the $(j-1)$th point sources, respectively]. Here S represents the source plane, D1 and D2 are two detectors.

to the detectors. Note that these two-photon amplitudes are of the same temporally random phase $(\phi_1+\phi_2)$, and therefore the interference term between the two paths will survive in an ensemble average. It is these twin two-photon paths that play an essential role in the two-photon interference with the phase-independent source. Recent advances also show that more than two indistinguishable two-photon paths could be introduced through interferometer [20] or phase control [21], leading to novel HBT-type two-photon interference effects.

Here we propose a two-photon interference scheme for classical light, where multiple NOON-type two-photon paths are introduced. This is realized through a specially designed classical source composed of many point sources j $(j=1,2,3,\ldots)$, and the complex amplitude of the point source j is proportional to $e^{i\phi_j}+e^{i\phi_j^{(1)}}$, a superposition of two modes, $e^{i\phi_j}$ and $e^{i\phi_j^{(1)}}$. Note that phases ϕ_j and $\phi_j^{(1)}$ are designed to change with time randomly but meet the condition $\phi_j+\phi_j^{(1)}=\phi_0$, in which ϕ_0, either a constant or a temporally random phase, is the same for all point sources. We emphasize here that two-photon measurement is done with the two detectors located at the same space point as required in a practical subwavelength interference scheme without postselected operation.

Now, let's consider the two-photon paths that contribute to the two-photon interference with such a source. In this case, two different types of two-photon paths need to be considered. The first type is the well-known HBT-type twin two-photon paths, as depicted in Fig. 1(a), where the pair of photons occupy two modes from two different point sources and their amplitudes are always in phase since two-photon measurement is done with the two detectors located at the same position. Therefore superposition of these twin two-photon paths only contributes a constant background to the two-photon interference. The second type is the NOON-type two-photon paths where the pair of photons occupy two modes of the same point source, as shown in Fig. 1(b). All NOON-type two-photon paths from different point sources j are indistinguishable since their amplitudes are of the same random phase $\phi_j+\phi_j^{(1)}=\phi_0$. Note that these NOON-type two-photon paths, with each path associated with a point source j, has the same two-photon interference scheme as that of the entangled two-photon source to realize subwavelength quantum lithography [6]. Therefore, if an object is put in front of the source plane and two-photon measurement is done, interference among these NOON-type two-photon paths will lead to subwavelength interference of the object. Since the subwavelength interference term originates only from the NOON-type (therefore entangled) two-photon paths, we could view the designed source as an effective entangled two-photon source.

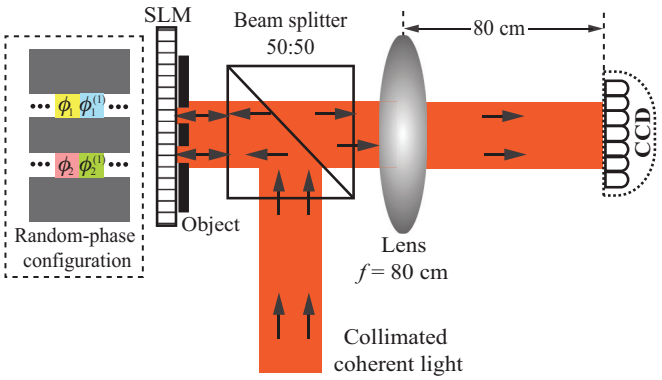

FIG. 2. (Color online) Diagram of the experimental setup. The inset on the left side shows the spatial configuration of the random-phase pairs on the slits of the mask.

III. EXPERIMENTAL DEMONSTRATION

To realize such an effective entangled two-photon source, one can use a spatial light modulator (SLM) to modulate the wave front of a coherent light according to the requirement $(e^{i\phi_j}+e^{i\phi_j^{(1)}})$ at the position of point source j. In our proof-of-principle experiment, we used a phase-only SLM to construct the source, where each point source j consisted of a pair of neighboring SLM pixels loaded with the random-phase pairs $(\phi_j,\phi_j^{(1)})$.

The diagram of our experimental setup is shown in Fig. 2. We expanded and collimated a single-mode laser with a wavelength of 780 nm (not shown in Fig. 2). The collimated coherent light was reflected by a 50:50 beam splitter and was then transmitted through an object (a double-slit mask with a slit width $a=72$ μm and a distance $d=400$ μm between the two slits) and was incident normally on a phase-only reflection-type SLM put right behind the object. The SLM was loaded with the random-phase pairs $(\phi_j,\phi_j^{(1)})$ at its jth pair of neighboring pixels, in which ϕ_j and $\phi_j^{(1)}$ are randomly and uniformly distributed within $[0,2\pi]$. In our experiment, we only loaded a pair of random phases $(\phi_m,\phi_m^{(1)})$ $(m=1,2)$ on each slit m of the double-slit mask, which is the simplest situation. To make sure the random-phase pair $(\phi_m,\phi_m^{(1)})$ has been encoded on the wave front of the light transmitting through the mth slit, we loaded the random-phase pair repeatedly along the mth slit, as shown in the inset of Fig. 2. In this way, the light reflected from the SLM worked as the effective entangled source, which transmitted through the object again and then was collected by a lens with a focal length $f=80$ cm. A CCD camera was put at the focal plane of the lens to measure the far-field single- and two-photon interference of the object.

For comparison, we first did not load any electric signal on the SLM, and the SLM worked as a reflection mirror. In this case, our experimental setup is the same as Yang's double-slit

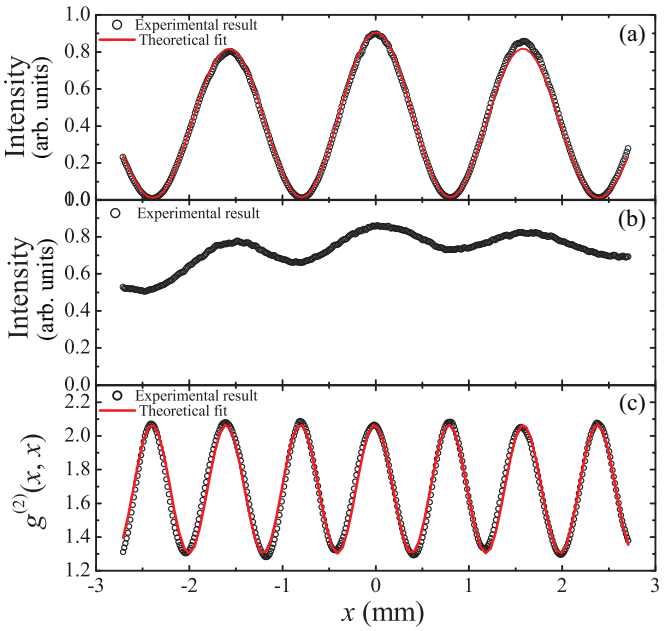

FIG. 3. (Color online) (a) Single-photon interference for the double-slit mask with a coherent light. (b) The measured intensity distribution in the far-field plane with the effective entangled source. (c) Two-photon interference for the double-slit mask with the effective entangled source.

interference setup. With a collimated coherent light, the far-field intensity distribution of the light field diffracted from the double-slit mask is $I(x) \propto \mathrm{sinc}^2[\pi a x/(\lambda f)]\{1 + y_1 \cos[2\pi d x/(\lambda f)]\}$, where y_1 represents the visibility of the interference fringes and λ is the wavelength. Figure 3(a) shows the experimental result (empty circles), with the solid curve being the theoretical fit. It represents typical single-photon interference fringes of the double-slit mask with the measured fringe period of 1.59 mm and $y_1 = 0.97$.

Next, let's turn to the situation when pairs of random phases were encoded on the wave front of the coherent light via the SLM. In this case, the light reflected from the SLM behaves as the effective entangled source. With such an effective entangled source, the light field diffracted from the double-slit mask will not show stationary single-photon interference fringes since the phase difference between the light beams transmitting through the two slits is randomly fluctuating in time. Figure 3(b) shows the average intensity distribution measured by the CCD camera with 10 000 realizations of the random-phase structure encoded on the wave front through the SLM. One can see that the first-order coherence is effectively erased in the experiment. The residual intensity peaks in Fig. 3(b) are caused by the phase flicker of the SLM during each realization of the random phases, which leads to partial first-order coherence of diffracted lights from the two slits.

Meanwhile, the two-photon interference effect of the double-slit mask was measured with the effective entangled source. Here, the normalized second-order correlation function $g^{(2)}(x,x) = \langle I(x,t)I(x,t)\rangle/[\langle I(x,t)\rangle\langle I(x,t)\rangle]$ was calculated by using 10 000 frames of the instantaneous intensity distributions measured by the CCD camera, corresponding to 10 000 realizations of the random-phase pairs encoded on the wave front of light. The experimental result (empty circles) is shown in Fig. 3(c). One sees that the two-photon interference pattern can be perfectly described as $g^{(2)}(x,x) \propto 1 + y_2 \cos[2\pi d x/(\lambda' f)]$ (solid curve) with $y_2 = 0.23$ being the fringe visibility and $\lambda' = 390$ nm being the effective wavelength, which is half of the wavelength (780 nm) of the laser source. Obviously, subwavelength interference of the double-slit mask is achieved with the effective entangled source.

IV. THEORETICAL CALCULATION

To theoretically confirm that subwavelength interference of an object could be realized through two-photon interference with the effective entangled source, the second-order spatial correlation function of the light field diffracted from the object needs to be calculated.

For comparison, let's first consider the traditional single-photon interference of the object with a collimated single-mode coherent light illuminating it. For simplicity, we consider the single-photon interference of the object in the far field (Fraunhofer zone) when a lens is put behind the object. By considering the aperture function $t(x_0)$ introduced by the object, the amplitude of the electromagnetic field in the far-field plane in one dimension can be expressed as [1]

$$E(x) \propto \int t(x_0)\psi(\lambda,x,x_0)dx_0\,, \tag{1}$$

where x_0 and x are the coordinates on the source plane and the far-field plane, respectively. $\psi(\lambda,x,x_0)$ is the propagation function in the far-field zone, which equals $e^{-i2\pi x x_0/(\lambda f)}$ in paraxial approximation. Here, f is the focal length of the lens, and λ is the wavelength of the incident coherent light. Then, one can get the intensity in the far-field plane as

$$I(x) = |E(x)|^2 \propto \left|\int t(x_0)\psi(\lambda,x,x_0)dx_0\right|^2, \tag{2}$$

which shows the far-field single-photon interference of the object with the aperture function $t(x_0)$. It can be seen that the resolution of the interference pattern is dependent on the wavelength λ.

Now, let's turn to the case when the object is illuminated by the effective entangled source. The amplitude of the far-field light field transmitting through the object can be expressed as

$$E(x) \propto \int \left(e^{i\phi(x_0)} + e^{i\phi^{(1)}(x_0)}\right)t(x_0)\psi(\lambda,x,x_0)dx_0\,. \tag{3}$$

The first-order spatial correlation function, i.e., the intensity on the far-field plane, can be derived as

$$\begin{aligned}\Gamma^{(1)}(x,x) &= \langle E^*(x)E(x)\rangle \\ &\propto \int \left\langle\left(e^{-i\phi(x_0)} + e^{-i\phi^{(1)}(x_0)}\right)\left(e^{i\phi(x_0')} + e^{i\phi^{(1)}(x_0')}\right)\right\rangle \\ &\quad \times t^*(x_0)t(x_0')\psi^*(\lambda,x,x_0)\psi(\lambda,x,x_0')dx_0dx_0' \\ &\propto 2\int |t(x_0)|^2|\psi(\lambda,x,x_0)|^2dx_0 \\ &\propto 2\int |t(x_0)|^2dx_0\,,\end{aligned} \tag{4}$$

where $\langle\cdots\rangle$ denotes the ensemble average and we have taken the conditions $\phi(x_0)+\phi^{(1)}(x_0)=\phi_0$ and $\langle e^{i\phi(x_0)}\rangle = \langle e^{i\phi^{(1)}(x_0)}\rangle = 0$ into account. It is easy to find that no stationary single-photon interference of $t(x_0)$ will emerge since the designed source is spatially first order incoherent.

Next, let's consider the second-order spatial correlation function, which can be expressed as

$$\begin{aligned}\Gamma^{(2)}(x,x) &= \langle E^*(x)E^*(x)E(x)E(x)\rangle \\ &\propto \int \left\langle \left(e^{-i\phi(x_0)}+e^{-i\phi^{(1)}(x_0)}\right)\left(e^{-i\phi(x_0')}+e^{-i\phi^{(1)}(x_0')}\right)\left(e^{i\phi(x_0'')}+e^{i\phi^{(1)}(x_0'')}\right)\left(e^{i\phi(x_0''')}+e^{i\phi^{(1)}(x_0''')}\right)\right\rangle \\ &\quad\times t^*(x_0)t^*(x_0')t(x_0'')t(x_0''')\psi^*(\lambda,x,x_0)\psi^*(\lambda,x,x_0')\psi(\lambda,x,x_0'')\psi(\lambda,x,x_0''')dx_0dx_0'dx_0''dx_0'''. \end{aligned} \tag{5}$$

There are 16 terms in $\langle\cdots\rangle$. Again, by considering $\phi(x_0)+\phi^{(1)}(x_0)=\phi_0$, $\langle e^{i\phi(x_0)}\rangle = \langle e^{i\phi^{(1)}(x_0)}\rangle = 0$, and terms such as $\langle e^{-i[\phi(x_0)+\phi(x_0')-\phi(x_0'')-\phi^{(1)}(x_0''')]}\rangle = 0$, the second-order correlation function can be simplified as

$$\begin{aligned}\Gamma^{(2)}(x,x) &\propto 8\left(\int |t(x_0)|^2|\psi(\lambda,x,x_0)|^2dx_0\right)^2 + 4\left|\int t^2(x_0)\psi^2(\lambda,x,x_0)dx_0\right|^2 \\ &\propto 8\left(\int |t(x_0)|^2dx_0\right)^2 + 4\left|\int t^2(x_0)\psi(\lambda/2,x,x_0)dx_0\right|^2. \end{aligned} \tag{6}$$

Note that the first term of Eq. (6) is the result of superposition of those twin HBT-type two-photon paths, which only contributes a constant background in this case. Interestingly, the interference between the NOON-type two-photon paths leads to the second term, which is characterized by an effective propagation function $\psi(\lambda/2,x,x_0)$ with a wavelength of $\lambda/2$. By comparing it with Eq. (2), one can easily find that the second term shows subwavelength interference of the object with a two-photon de Broglie wavelength of $\lambda/2$.

V. DISCUSSIONS

It is not difficult to find out that our experiment is a NOON-type two-photon interference scheme, different from the HBT-type experiment [10,22]. In general, the normalized second-order correlation function $g^{(2)}(x_1,x_2)$ is measured at two different positions (x_1, x_2) and will be a constant when $x_1=x_2$ in the conventional HBT-type experiment. However, in our experiment, we measured $g^{(2)}(x,x)$, where $x_1=x_2=x$, and $g^{(2)}(x,x)$ shows subwavelength interference with respect to x without any postselection operation. This is because the two-photon interference scheme as shown in Fig. 1(a) plays a key role in the HBT-type experiment, while multiple entangled two-photon paths as shown in Fig. 1(b) play an essential role in our experiment. Note that subwavelength interference of $g^{(2)}(x,x)$ was also observed recently by Cao *et al.* [11] in a modified HBT-type setup by inserting an incoherent interferometer which is composed of two orthogonally polarized imaging arms: one is a $2f-2f$ imaging system and the other contains two $2f'-2f'$ imaging systems. Since the $2f-2f$ imaging system reverses the input wave front while the two $2f'-2f'$ imaging systems keep it in the imaging plane, the intensity correlation between a pair of symmetric positions at the input port of the incoherent interferometer is transferred to the correlation of the same position between two orthogonally polarized modes at the output port. It is evident that the two-photon path scheme of the modified HBT-type setup is essentially the same as that shown in Fig. 1(a), which is inherently different from the NOON-type one shown in Fig. 1(b).

When one takes a deep look into the entangled two-photon paths here, one may note that they somehow look different from the two entangled paths A and B of the quantum NOON state, i.e., $(|N,0\rangle_{A,B}+|0,N\rangle_{A,B})/\sqrt{2}$. In the quantum regime, the two photons detected by the detectors are in the Fock states. However, in our entangled two-photon path scheme, the detected photons are from a coherent state. The trick to obtain the quantum-like entangled two-photon paths here relies on the designed mode-superposed point sources, which provide multiple pairs of coupled modes $e^{i\phi_j}$ and $e^{i\phi_j^{(1)}}$ ($j=1,2,3,\ldots$). It is the superposition of these pairs of the coupled modes that finally contributes to the subwavelength interference.

The NOON-type two-photon interference was discussed and demonstrated previously by employing nonlinear processes such as parametric scattering, the spontaneous parametric down-conversion effect, and two-photon atomic transition, whether in quantum or classical regimes [23]. Consequently, the spatial resolution of the observed two-photon subwavelength interference is actually the same as that of the single-photon interference of the pump beam [6]. In our case, the NOON-type two-photon subwavelength interference is achieved in a linear system simply employing a coherent light and a spatial light modulator, and the spatial resolution is indeed increased by a factor of 2 compared to that of the single-photon interference of the incident coherent beam. In addition, our NOON-type two-photon subwavelength interference is achieved without postselection, in which the two detectors are at the same spatial point as required by practical applications. Although the visibility is relatively low for classical light compared to the case with a quantum entangled two-photon source, our scheme provides the advantages of having higher intensity and being more easily achievable, which are useful for applications such as optical lithography based on the photonic de Broglie wave.

VI. SUMMARY

In summary, by introducing an effective entangled two-photon source, quantum-like entangled two-photon paths are introduced through multiple pairs of coupled modes $(e^{i\phi(x_0)}, e^{i\phi^{(1)}(x_0)})$. The two photons associated with the entangled two-photon paths behave as a whole one with a de Broglie wavelength half of that of the original incident coherent light. With such a source, subwavelength interference of an object, which is put in front of the source plane, can be achieved via two-photon measurement. In a proof-of-principle experiment, we have observed second-order subwavelength interference of a double-slit mask. The result shows a way to realize the photonic de Broglie wave with a classical light in a linear system.

ACKNOWLEDGMENTS

This work is supported by the 973 program (Grant No. 2013CB328702), the NSFC (Grant No. 11174153), and the 111 project (Grant No. B07013).

[1] G. Brooker, *Modern Classical Optics* (Oxford University Press, Oxford, 2003).
[2] J. Jacobson, G. Bjork, I. Chuang, and Y. Yamamoto, Phys. Rev. Lett. **74**, 4835 (1995).
[3] E. J. S. Fonseca, C. H. Monken, and S. Pádua, Phys. Rev. Lett. **82**, 2868 (1999).
[4] K. Edamatsu, R. Shimizu, and T. Itoh, Phys. Rev. Lett. **89**, 213601 (2002).
[5] A. N. Boto, P. Kok, D. S. Abrams, S. L. Braunstein, C. P. Williams, and J. P. Dowling, Phys. Rev. Lett. **85**, 2733 (2000).
[6] M. D'Angelo, M. V. Chekhova, and Y. Shih, Phys. Rev. Lett. **87**, 013602 (2001).
[7] M. W. Mitchell, J. S. Lundeen, and A. M. Steinberg, Nature (London) **429**, 161 (2004).
[8] P. Walther, J. Pan, M. Aspelmeyer, R. Ursin, S. Gasparoni, and A. Zeilinger, Nature (London) **429**, 158 (2004).
[9] I. Afek, O. Ambar, and Y. Silberberg, Science **328**, 879 (2010).
[10] J. Xiong, D. Z. Cao, F. Huang, H. G. Li, X. J. Sun, and K. Wang, Phys. Rev. Lett. **94**, 173601 (2005).
[11] D. Cao, G. Ge, and K. Wang, Appl. Phys. Lett. **97**, 051105 (2010).
[12] A. Pe'er, B. Dayan, M. Vucelja, Y. Silberberg, and A. A. Friesem, Opt. Express **12**, 6600 (2004).
[13] P. R. Hemmer, A. Muthukrishnan, M. O. Scully, and M. S. Zubairy, Phys. Rev. Lett. **96**, 163603 (2006).
[14] K. J. Resch, K. L. Pregnell, R. Prevedel, A. Gilchrist, G. J. Pryde, J. L. O'Brien, and A. G. White, Phys. Rev. Lett. **98**, 223601 (2007).
[15] C. Thiel, T. Bastin, J. Martin, E. Solano, J. von Zanthier, and G. S. Agarwal, Phys. Rev. Lett. **99**, 133603 (2007).
[16] U. Fano, Am. J. Phys. **29**, 539 (1961).
[17] L. Mandel, Rev. Mod. Phys. **71**, S274 (1999).
[18] A. Nevet, A. Hayat, P. Ginzburg, and M. Orenstein, Phys. Rev. Lett. **107**, 253601 (2011).
[19] J. Liu and G. Zhang, Phys. Rev. A **82**, 013822 (2010).
[20] P. Hong, J. Liu, and G. Zhang, Phys. Rev. A **86**, 013807 (2012).
[21] P. Hong, L. Xu, Z. Zhai, and G. Zhang, Opt. Express **21**, 14056 (2013).
[22] R. Hanbury Brown and R. Q. Twiss, Nature (London) **177**, 27 (1956); **178**, 1046 (1956).
[23] A. V. Belinskii and D. N. Klyshko, Phys. Usp. **36**, 653 (1993).